

Focal adhesion kinase

An alternative focus for anti-angiogenesis therapy in ovarian cancer

Rebecca L Stone¹, Keith A Baggerly², Guillermo N Armaiz-Pena¹, Yu Kang³, Angela M Sanguino¹, Duangmani Thanappapas¹, Heather J Dalton¹, Justin Bottsford-Miller¹, Behrouz Zand¹, Rehan Akbani², Lixia Diao², Alpa M Nick¹, Koen DeGeest⁴, Gabriel Lopez-Berestein⁵, Robert L Coleman¹, Susan Lutgendorf⁶, and Anil K Sood^{1,7,*}

¹Department of Gynecologic Oncology; The University of Texas M.D. Anderson Cancer Center; Houston, TX USA; ²Department of Bioinformatics and Computational Biology; The University of Texas M.D. Anderson Cancer Center; Houston, TX USA; ³Department of Obstetrics and Gynecology; Hospital of Fudan University; Shanghai, PR China; ⁴Department of Obstetrics and Gynecology; The University of Iowa; Iowa City, IA USA; ⁵Department of Experimental Therapeutics; The University of Texas M.D. Anderson Cancer Center; Houston, TX USA; ⁶Department of Psychology; The University of Iowa; Iowa City, IA USA; ⁷Department of Cancer Biology; The University of Texas M.D. Anderson Cancer Center; Houston, TX USA

Keywords: angiogenesis, metastasis, cancer/molecular biology, targeted therapy

Abbreviations: FAK, focal adhesion kinase; EOC, epithelial ovarian cancer; FAK-T, tumor cell FAK; pFAK-T, tumor cell phospho-FAK; FAK-endo, tumor-associated endothelial cell FAK; pFAK-endo, tumor-associated endothelial cell phospho-FAK; MVD, microvessel density; VEGF, vascular endothelial cell growth factor; TCGA, The Cancer Genome Atlas; CBS, circular binary segmentation; RMA, Robust Microchip Algorithm; HUVEC, human umbilical vein endothelial cells; CGH, comparative genomic hybridization

This investigation describes the clinical significance of phosphorylated focal adhesion kinase (FAK) at the major activating tyrosine site (Y397) in epithelial ovarian cancer (EOC) cells and tumor-associated endothelial cells. FAK gene amplification as a mechanism for FAK overexpression and the effects of FAK tyrosine kinase inhibitor VS-6062 on tumor growth, metastasis, and angiogenesis were examined. FAK and phospho-FAK^{Y397} were quantified in tumor (FAK-T; pFAK-T) and tumor-associated endothelial (FAK-endo; pFAK-endo) cell compartments of EOCs using immunostaining and qRT-PCR. Associations between expression levels and clinical variables were evaluated. Data from The Cancer Genome Atlas were used to correlate FAK gene copy number and expression levels in EOC specimens. The in vitro and in vivo effects of VS-6062 were assayed in preclinical models. FAK-T and pFAK-T overexpression was significantly associated with advanced stage disease and increased microvessel density (MVD). High MVD was observed in tumors with elevated endothelial cell FAK (59%) and pFAK (44%). Survival was adversely affected by FAK-T overexpression (3.03 vs 2.06 y, $P = 0.004$), pFAK-T (2.83 vs 1.78 y, $P < 0.001$), and pFAK-endo (2.33 vs 2.17 y, $P = 0.005$). FAK gene copy number was increased in 34% of tumors and correlated with expression levels ($P < 0.001$). VS-6062 significantly blocked EOC and endothelial cell migration as well as endothelial cell tube formation in vitro. VS-6062 reduced mean tumor weight by 56% ($P = 0.005$), tumor MVD by 40% ($P = 0.0001$), and extraovarian metastasis ($P < 0.01$) in orthotopic EOC mouse models. FAK may be a unique therapeutic target in EOC given the dual anti-angiogenic and anti-metastatic potential of FAK inhibitors.

Introduction

Epithelial ovarian cancer is the fifth leading cause of cancer death among US women and is the most lethal gynecologic malignancy. Unfortunately, mortality rates have not appreciably decreased over the past decade largely because recurrent platinum-resistant ovarian cancer remains incurable. While improvements in clinical outcome have been achieved with VEGF inhibitors, disease control with these agents remains finite.¹ To date, the majority of studies have focused more on how well anti-angiogenic treatment blocks target lesion growth and less on metastasis. However, given the recent observation that tumors may elicit

evasive resistance marked by increased metastasis in response to VEGF inhibition, investigation of agents with combined anti-angiogenic and anti-metastatic activity is needed.² This study examines the unique therapeutic potential of focal adhesion kinase (FAK) inhibitors to induce dual anti-angiogenic and anti-metastatic effects in preclinical models of ovarian cancer.

Focal adhesion kinase is a non-receptor tyrosine kinase that functions as a central node in signaling networks arising from focal adhesions. Focal adhesions are multi-protein complexes that mediate cell contact with the extracellular matrix (ECM) and relay information between the ECM and the cell cytoplasm.^{3,4} Thus, FAK interfaces cells with their microenvironment.

*Correspondence to: Anil K Sood; Email: asood@mdanderson.org

Submitted: 01/05/2014; Revised: 04/13/2014; Accepted: 04/13/2014; Published Online: 04/23/2014
<http://dx.doi.org/10.4161/cbt.28882>

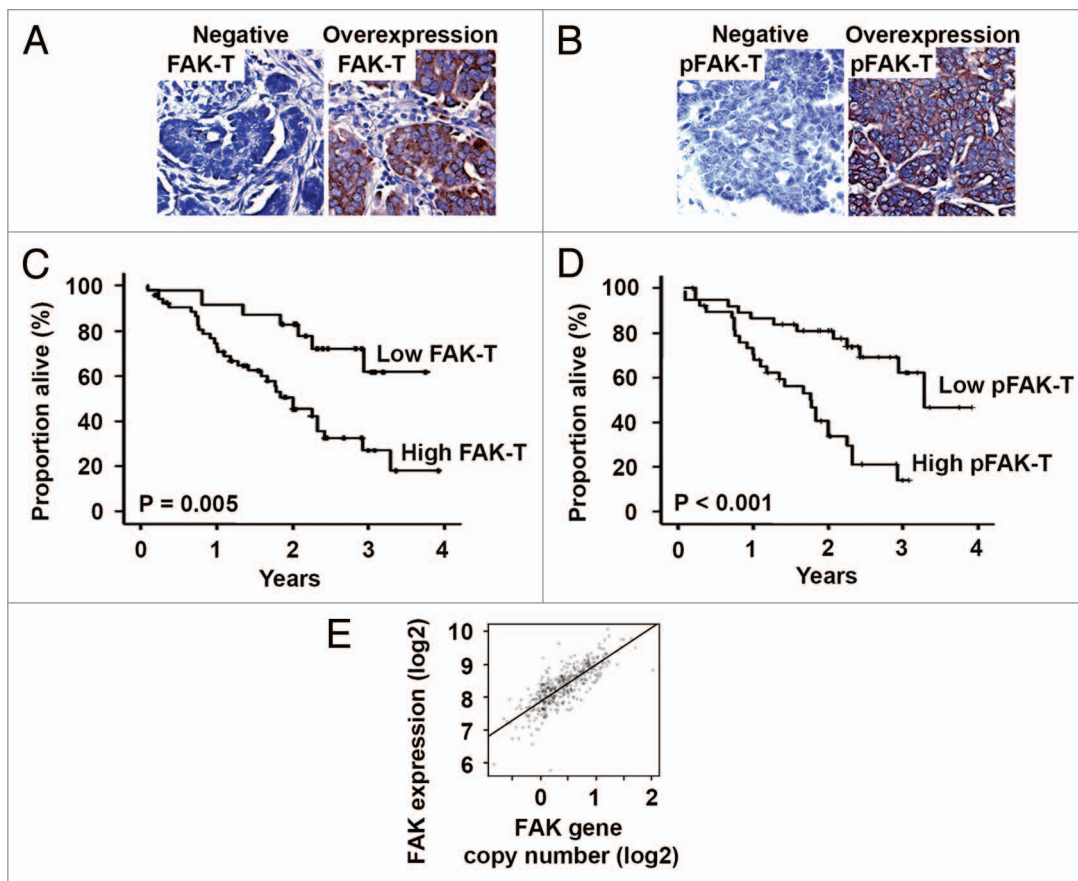


Figure 1. Tumor cell FAK and pFAK^{Y397} expression in human epithelial ovarian cancer. (A) Representative tumor cell FAK (FAK-T) immunohistochemical staining in advanced stage, high grade serous ovarian cancer specimens. Negative FAK-T expression and FAK-T overexpression are represented in the left and right panels, respectively. (B) Representative tumor cell pFAK^{Y397} (pFAK-T) immunohistochemical staining in advanced stage, high grade serous ovarian cancer specimens. Negative pFAK-T expression and pFAK-T overexpression are represented in the left and right panels, respectively. Images were captured at original magnification 200x. (C) Kaplan–Meier plot depicting the impact of tumor cell FAK (FAK-T) expression on ovarian cancer patient survival using the log-rank statistic. (D) Kaplan–Meier plot depicting the impact of tumor cell pFAK^{Y397} (pFAK-T) expression on ovarian cancer patient survival using the log-rank statistic. (E) Correlation between FAK gene copy number and mRNA expression levels determined in human epithelial ovarian cancers using CGH arrays and Affymetrix U133A expression arrays, respectively.

Although FAK predominantly controls integrin-mediated signal transduction, accumulating evidence indicates that FAK activation also occurs in response to diverse stimuli including growth factors, phospholipids, neuropeptides, and cytokines.⁵ Engagement of integrins and numerous other receptors results in FAK autophosphorylation at tyrosine residue 397 (pFAK^{Y397}), which is the most critical site for kinase activation.⁶ FAK activation initiates a cascade of signaling events that promote cell survival, proliferation, migration, invasion, and angiogenesis.⁷ Thus, FAK scaffolding and kinase activity control cell functions that fundamentally become deregulated in the course of malignant progression including pro-angiogenic endothelial cell behaviors.⁸ We have previously demonstrated that FAK mRNA and protein levels are elevated in epithelial ovarian cancer.^{9,10} While mechanistic data explaining this observation are lacking, it is noteworthy that amplification of 8q, where FAK gene is located (8q24.3), is one of the most frequent genetic alterations in primary ovarian cancers and is associated with poorly differentiated tumors.^{11,12}

Thus, FAK gene amplification could be an important mechanism for high FAK in ovarian cancer. Evidence of this genetic link to FAK protein overexpression would strengthen the rationale for targeting FAK in this particular malignancy. Given the emergence of small molecule inhibitors that target FAK catalytic activity (e.g., TAE226, Novartis Inc.; VS-6062/PF-562,271, Verastem/Pfizer; PF-573,228, Pfizer; defactinib/VS-6063, Verastem; VS-4718, Verastem; GSK2256098, GlaxoSmithKline; BI 853520 Boehringer Ingelheim)^{13–19} and limited information regarding FAK activation in ovarian cancer, we conducted the current investigation to evaluate the expression, clinical significance, and anti-tumor effects of inhibiting FAK phosphorylation at the major activating tyrosine site (Y397) in epithelial ovarian cancer cells and tumor-associated endothelial cells. Additionally, we ascertained whether changes in FAK gene copy number track with changes in expression using data available through The Cancer Genome Atlas (TCGA) in order to gain mechanistic understanding of increased FAK expression in ovarian cancer.

Table 1. Correlation of clinicopathologic variables with epithelial ovarian cancer tumor cell (-T) FAK and pFAK expression

Variable	FAK-T		P value	pFAK-T		P value
	No	Yes		No	Yes	
<i>Stage</i>						
Low (I-II)	9	3	< 0.001	11	1	0.002
High (III-IV)	16	52		29	39	
<i>Grade</i>						
Low (I)	5	3	0.044	6	2	0.14
High (II-III)	20	52		34	38	
<i>Histology</i>						
Serous	22	48	0.93	32	38	0.04
Other	3	7		8	2	
<i>MVD*</i>						
Low	10	10	0.04	16	4	0.002
High	15	45		24	36	
<i>Cytoreduction</i>						
Optimal	8	22	0.49	13	17	0.36
Suboptimal	17	33		27	23	

*MVD, microvessel density.

Results

FAK and pFAK^{Y397} expression in epithelial ovarian cancer cells

First, the tumor cells were evaluated for FAK (FAK-T) and pFAK^{Y397} (pFAK-T) expression by immunohistochemistry in 80 epithelial ovarian cancers. Consistent with our previous findings, FAK-T overexpression was observed in 69% of cases (Fig. 1A). Overexpression of pFAK-T was identified in 50% of cases (Fig. 1B). There was a strong link between FAK-T and pFAK-T expression levels ($P < 0.01$). Correlations between clinicopathological variables and tumor cell FAK and pFAK expression are summarized in Table 1. FAK-T overexpression was associated with advanced stage ($P < 0.001$) and high grade ($P = 0.044$) disease. FAK-T overexpression was found in 25% and 77% of ovarian cancers limited to (stage I/II) and spread beyond (stage III/IV) the pelvis, respectively. Overexpression of pFAK-T was also significantly associated with disease dissemination; high pFAK-T levels were detected in 57% of stage III/IV compared with only 8% of stage I/II ovarian cancers ($P = 0.002$). On the basis of finding strong associations between FAK-T and pFAK-T expression and stage, we examined the effect of expression levels on patient survival. Mean overall survival among patients with FAK-T overexpression was 2.16 y, compared with 3.06 y for patients with low FAK-T expression ($P = 0.005$, Fig. 1C). Survival was also adversely affected by pFAK-T overexpression. Mean overall survival was 3.04 vs. 1.81 y for patients with low and high pFAK-T expression, respectively ($P < 0.001$, Fig. 1D).

Relationship between FAK gene copy number and expression in ovarian cancer

Based on finding FAK overexpression and activation to portend poor prognosis, we investigated the underlying mechanism

of increased FAK protein expression in this malignancy. Several recent reports characterizing recurrent chromosomal aberrations in ovarian cancer have revealed a high frequency of gains in 8q, the chromosomal locus of the FAK gene. These data prompted us to investigate the presence of FAK gene amplification and whether changes in FAK copy number track with changes in gene expression in a subset of ovarian cancers. Using a circular binary segmentation (CBS) cutoff of 0.5, we detected increases in FAK copy number in 13 of the 38 tumors evaluated. Recurrent loss of 8p was also observed. This aberration was not detected in any of the benign ovaries we examined ($n = 10$); the magnitude of all CBS values was less than 0.05.

The correlation between the two Affymetrix probes targeting FAK was high ($r = 0.78$). The correlation between FAK CBS levels and gene expression levels was statistically significant using either probeset 208820_at ($\rho = 0.61$, $P = 3.7e-06$) or probeset 207821_s_at ($\rho = 0.40$, $P = 0.0054$). Fitting a regression model using CBS value to predict expression levels of 208820_at gave a slope coefficient of 0.76 and a multiple R-squared of 0.36 ($P = 6.5e-05$). Thus, unit increase in CBS value would lead us to predict an increase of 0.76 units in the Robust Multichip Algorithm (RMA) value (Fig. 1E).

Relationship of ovarian cancer cell FAK and pFAK^{Y397} expression to angiogenesis

There are emerging data that FAK is a key mediator of angiogenesis.^{20,21} To explore the relationship between ovarian cancer cell FAK and pFAK expression and the tumor vasculature, we stained the specimens for CD31 and quantified microvessel density (MVD). The median MVD was 21.6 vessels/high power field (range, 8.6–38.3 vessels/high power field). High FAK-T expression and activation (pFAK-T) were significantly associated with high MVD ($P = 0.04$ and $P = 0.002$). It is well-established

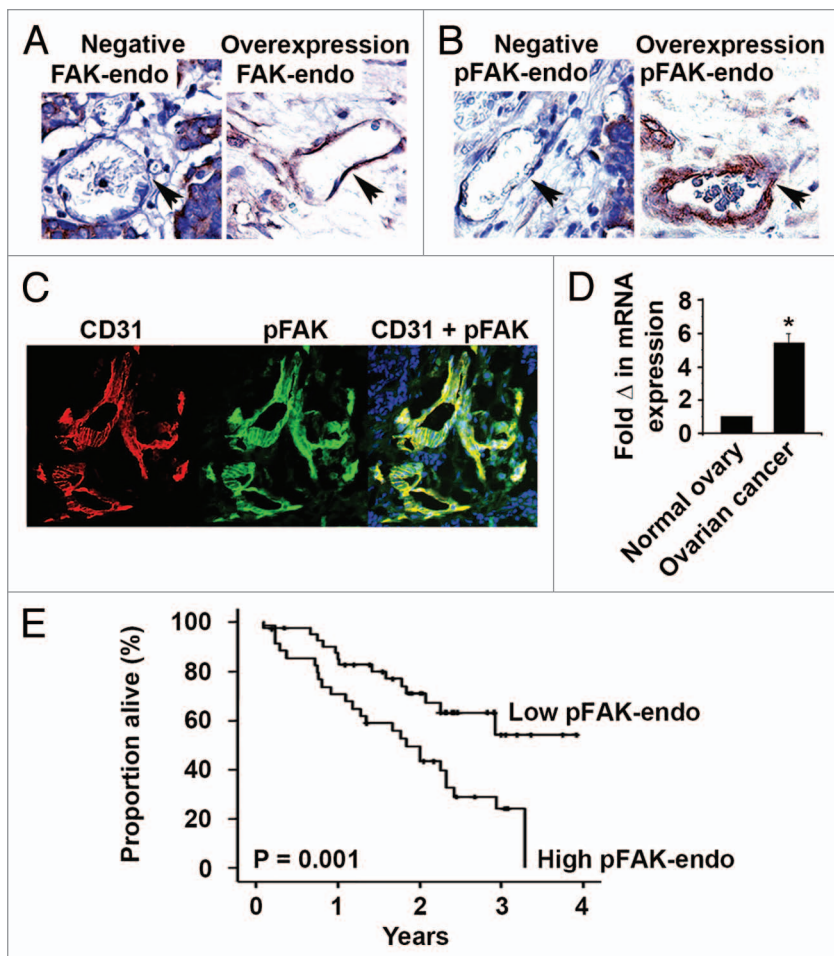


Figure 2. Tumor-associated endothelial cell FAK and pFAK^{Y397} expression in human epithelial ovarian cancer. (A) Representative tumor-associated endothelial cell FAK (FAK-endo) immunohistochemical staining in advanced stage, high grade serous ovarian cancer specimens. Negative FAK-endo expression and FAK-endo overexpression are represented in the left and right panels, respectively. (B) Representative tumor-associated endothelial cell pFAK^{Y397} (pFAK-endo) immunohistochemical staining in advanced stage, high grade serous ovarian cancer specimens. Negative pFAK-endo expression and pFAK-endo overexpression are represented in the left and right panels, respectively. Images were captured at original magnification 200 \times . (C) Representative CD31 (left panel) and pFAK^{Y397} (center panel) immunofluorescent staining in advanced stage, high grade serous ovarian cancer. Dual CD31 and pFAK^{Y397} staining (right panel) demonstrates activated FAK in the tumor vasculature. Images were captured at original magnification 200 \times . (D) Quantitative real-time PCR of endothelial cell FAK expression. FAK gene expression in 10 ovarian cancer isolates was calculated as the mean fold change relative to 7 normal ovarian endothelial specimens (normal = 1) using the $2^{-\Delta\Delta C_t}$ method. (E) Kaplan–Meier plot depicting the impact of tumor-associated endothelial cell pFAK^{Y397} (pFAK-endo) expression on ovarian cancer patient survival using the log-rank statistic.

that high MVD is a poor prognostic factor in ovarian cancer.^{22,23} Consistent with this, MVD exceeding 12.7 vessels/HPF predicted poor overall survival (3.22 vs. 2.19 mean years, $P = 0.002$).

FAK and pFAK^{Y397} expression in ovarian cancer vasculature

Given the link between ovarian cancer cell FAK and tumor vascularity, as well as recent data pointing to a direct role for endothelial cell FAK in angiogenesis, we examined the clinical significance of tumor endothelial cell FAK (FAK-endo) and pFAK^{Y397} (pFAK-endo). We detected high FAK-endo and pFAK-endo

expression in 59% and 44% of cases, respectively (Figs. 2A and B). FAK-endo and pFAK-endo expression levels strongly correlated ($P < 0.01$). However, endothelial cell FAK expression and activation did not correlate with tumor cell FAK status. Activated FAK in the tumor vasculature was confirmed using immunofluorescence dual-labeling for CD31 and p-FAK (Fig. 2C). To validate our immunohistochemical detection of FAK overexpression in tumor-associated endothelial cells, we used quantitative real-time PCR to measure FAK transcript in endothelial cell isolates from normal ovary ($n = 7$) and ovarian carcinoma ($n = 10$). We detected a 5.4-fold increase in FAK transcript in tumor-associated endothelial cells compared with endothelial cells isolated from normal ovaries (Fig. 2D, $P < 0.01$).

Correlations between tumor-associated endothelial cell FAK and pFAK expression and clinicopathological variables are summarized in Table 2. FAK-endo and pFAK-endo expression significantly correlated with high MVD ($P = 0.01$ and $P = 0.001$). FAK-endo and pFAK-endo overexpression was detected in 65% and 53% of tumors with high MVD, respectively. Additionally, high FAK activation in the tumor-related vasculature was associated with poor overall survival. Mean overall survival was 1.86 y compared with 2.93 y for patients with and without activated FAK in tumor-associated endothelial cells ($P = 0.001$, Fig. 2E).

In vitro effects of FAK tyrosine kinase inhibitor VS-6062 on FAK phosphorylation, ovarian cancer cell proliferation and migration, and endothelial cell tube formation

Novel ATP-competitive small molecule inhibitors of FAK with improved specificity and bioavailability, such as VS-6062, are now emerging from drug development. To evaluate the therapeutic potential of VS-6062 using preclinical models of ovarian cancer, we first determined the dose and time kinetics of VS-6062 in blocking phosphorylation of the FAK Y397 activation site in vitro. Treatment of HeyA8 ovarian cancer cells with VS-6062 resulted in dose dependent inhibition of pFAK^{Y397} with pFAK^{Y397} blockade persisting for up to 12 h (Fig. 3A). HeyA8 cell viability was not affected by VS-6062 treatment until doses $\geq 0.1 \mu\text{M}$ were used, with an IC_{50} of 57.5 μM (Fig. 3B). Given that FAK integrates growth factor and integrin signals to promote cell migration, we tested the effect of VS-6062 on this endpoint. Treatment with the IC_{70} dose for FAK catalytic activity (0.5 μM) blocked HeyA8 migration by $> 50\%$ ($P < 0.001$, Fig. 3C). Since our clinical data suggest FAK is an important therapeutic target in both ovarian cancer tumor and endothelial cells, we also evaluated the effect of FAK inhibition on human

Table 2. Correlation of clinicopathologic variables with FAK and pFAK expression in endothelial cells (-endo) of epithelial ovarian cancers

Variable	FAK-endo		P value	pFAK-endo		P value
	No	Yes		No	Yes	
<i>Stage</i>						
Low (I-II)	5	7	0.97	9	3	0.16
High (III-IV)	28	40		36	32	
<i>Grade</i>						
Low (I)	3	5	0.82	5	3	0.71
High (II-III)	30	42		40	32	
<i>Histology</i>						
Serous	26	44	0.048	37	33	0.11
Other	7	3		8	2	
<i>MVD*</i>						
Low	12	8	0.04	17	3	0.003
High	21	39		28	32	
<i>Cytoreduction</i>						
Optimal	12	18	0.86	16	14	0.68
Suboptimal	21	29		29	21	

*MVD, microvessel density.

umbilical vein endothelial cell (HUVEC) migration and tube formation to assess the anti-angiogenic activity of VS-6062 in vitro. VS-6062 completely blocked VEGF-stimulated endothelial cell migration (Fig. 3D) and potently inhibited endothelial cell branched tube formation by > 70% ($P < 0.001$, Fig. 3E).

In vivo effects of FAK tyrosine kinase inhibitor VS-6062 on ovarian cancer growth, metastasis, and angiogenesis

To determine the in vivo therapeutic potential of VS-6062, we tested the effect of this inhibitor on tumor growth in the HeyA8 intraperitoneal mouse model of ovarian cancer. VS-6062 treatment reduced mean HeyA8 tumor weight by 56% and mean number of tumor implants by 55% ($P = 0.005$ and $P = 0.001$, Fig. 4A). Western blot for pFAK^{Y397} was used to confirm target modulation in tumors. VS-6062 decreased mean tumor pFAK^{Y397} levels by >80% ($P = 0.01$, Fig. 4B). Mean mouse weight did not differ between VS-6062 and control treated mice (22.6 vs. 22.3 g). Based on the clinical significance of endothelial pFAK^{Y397} and the ability of VS-6062 to inhibit endothelial tube formation in vitro, we assayed tumor MVD. VS-6062 treated tumors were significantly more avascular. Specifically, VS-6062 reduced tumor MVD by 40% compared with vehicle control ($P = 0.0001$, Fig. 4C), suggesting that the therapeutic potential of VS-6062 may be in part related to anti-angiogenic effects of FAK inhibition.

To better evaluate the anti-metastatic effects of VS-6062, we utilized a fully orthotopic mouse model generated by injecting SKOV3ip1 human ovarian cancer cells directly into the ovary. VS-6062 treatment reduced mean SKOV3ip1 tumor weight and intraperitoneal dissemination by 58% and 85%, respectively ($P < 0.001$, Fig. 4D). Further, we observed a significant decrease in site-specific extraovarian metastasis in VS-6062 treated animals ($P < 0.05$, Fig. 4E). Taken together, these findings suggest

that the therapeutic potential of FAK inhibitors may stem from dual anti-angiogenic and anti-metastatic activity.

Discussion

The key findings from this investigation are that elevated FAK protein expression and activation occur in both the tumor cells and tumor-associated vasculature of a substantial proportion of epithelial ovarian carcinomas. A strong link between FAK gene copy number and expression provides one mechanistic explanation for increased FAK in ovarian cancer. FAK and pFAK^{Y397} overexpression in ovarian cancer cells is significantly associated with advanced stage disease and compromised survival. Furthermore, high FAK activation in tumor and endothelial cells occurs in ovarian carcinomas with increased vascularity. Overexpression of pFAK^{Y397} in the tumor vasculature is also clinically relevant in portending poor prognosis. While FAK has been shown to control a wide range of cellular processes, our clinical data support a role for FAK in driving ovarian cancer metastasis and angiogenesis. Data from preclinical models of ovarian cancer evaluating the anti-tumor effects of FAK downregulation with small molecule inhibitor VS-6062 provide a biological basis for this. Tumor growth, spread, and angiogenesis were abrogated by VS-6062 induced FAK inhibition at the major auto-phosphorylation and activating Y397 site.

To our knowledge, this study is the first to add functional significance to newly emerging comparative genomic hybridization (CGH) analyses of ovarian cancer by acting on knowledge of 8q amplification to link increases in FAK expression to gene copy number gains. This association suggests that induced changes in FAK may be persistent as opposed to transient, further increasing

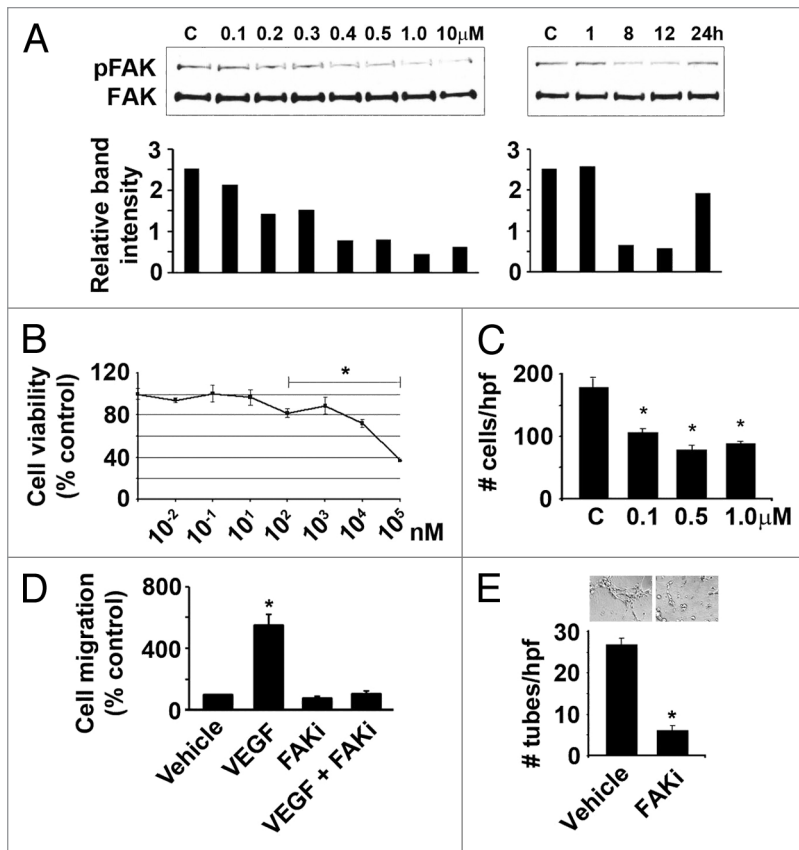


Figure 3. Effect of VS-6062 induced pFAK^{Y397} inhibition on ovarian cancer cell viability and migration as well as endothelial cell migration and tube formation. **(A)** Dose (left panel) and time (right panel) kinetics of VS-6062 induced inhibition of pFAK^{Y397} in HeyA8 ovarian cancer cells (c, vehicle control). HeyA8 cells were treated with 0.1–10 μ M VS-6062 for 8 h to examine VS-6062 dose dependent inhibition of pFAK^{Y397} by western blot. Time-kinetic experiments were performed to determine the onset and duration of action of VS-6062 in downregulating pFAK^{Y397}. Following treatment with 0.5 μ M of VS-6062, lysates were collected at 1, 8, 12, and 24 h and then analyzed for FAK phosphorylation at residue Y397 by western blot. Relative band intensity of pFAK relative to FAK corresponding to each dose/time point is plotted in the histograms below each panel. **(B)** Effect of increasing concentrations of VS-6062 on HeyA8 cell viability normalized to vehicle control. Points, means of three independent experiments \pm SE. **(C)** Effect of VS-6062 (0.1–1 μ M) on HeyA8 cell migration (c, vehicle control). Bars, mean number of migrated cells per high power field (HPF) \pm SE. **(D)** Effect of VS-6062 (0.5 μ M) on VEGF-A stimulated HUVEC migration. **(E)** Effect of VS-6062 (0.5 μ M) on HUVEC tube formation. Bars, mean number of tubes per high power field (HPF) \pm SE. Representative photomicrographs appear above the histogram. Images were captured at original magnification 100 \times . FAKi, FAK inhibitor VS-6062; Vehicle, equivalent DMSO in PBS diluent.

the appeal of FAK as a drug target. While FAK gene amplification may be a prominent mechanism underlying high FAK expression in ovarian cancer, FAK upregulation might also arise in response to epigenetic changes.²⁴ Recent analysis of the human FAK promoter identified binding sites for several transcription factors including p53.²⁵ However, the fact that p53 is mutated in nearly all serous ovarian adenocarcinomas (the most common histologic subtype), suggests that the mechanism for FAK expression in ovarian cancer is more complex than p53 status.^{26,27} There is some evidence to suggest that phosphatases, such as phosphatase and tensin homolog (PTEN), suppress FAK activation by dephosphorylation of tyrosine residues.²⁸ Thus, disruption of

PTEN, which can result from allelic loss, intragenic mutation, or epigenetic silencing in epithelial ovarian carcinoma, could contribute to high levels of FAK activation in this malignancy as well.²⁹

The recognition of FAK as a critical mediator of cellular motility combined with the reality that most cancer deaths are attributable to distant spread as opposed to local complications explains why the kinase has garnered increasing interest in clinical research.^{7,30} In fact, there is evidence that FAK operates at multiple points along the metastatic cascade. FAK signaling modulates changes in cell adhesion, motility, and invasion capabilities, homing to the metastatic target organ, and angiogenic switch activation.³¹ The strong association we identified between FAK activation and advanced stage disease is a clinical corollary of this. Our in vivo observation of reduced upper abdominal tumor involvement with FAK inhibition may also have clinical relevance. Large volume upper abdominal primary and recurrent ovarian cancer involving the diaphragm, liver, and/or spleen is a major obstacle to achieving optimal surgical cytoreduction.³² Furthermore, there are Gynecologic Oncology Group (GOG) data indicating that stage III ovarian cancer patients with initial disease in the upper abdomen have a worse prognosis despite cytoreductive surgery to microscopic residual, implying that factors beyond cytoreductive effort are important in predicting survival.³³ Whether differences in tumor biology, such as FAK upregulation, account for this remains unknown.

Some of the most provocative data implicate FAK in both physiologic and pathologic angiogenesis. FAK null embryos fail to develop vascular networks and endothelial FAK-deletion in adult mice impedes tumor growth by diminishing angiogenesis. In both settings it is apparent that endothelial FAK is an important mediator of VEGF-induced neovascularization.^{20,21} Taken together, these findings provide strong rationale for targeting FAK to simultaneously counter tumor metastasis and angiogenesis. To this end, there has been a surge in the discovery and pre-clinical development of agents directed against FAK. These approaches include the various small molecule inhibitors and FAK silencing using FAK targeted short interfering RNA (siRNA).^{34,35} Recently, VS-6062 was the first-in-class FAK inhibitor to enter phase I dose-escalation trials in advanced, terminal solid malignancies. Disease stability (\geq six 21 d cycles) was observed in 15 of 91 patients (16%) with measurable disease, which is noteworthy for a heavily pre-treated population.³⁶ Achievement of prolonged disease stabilization highlights the therapeutic potential of FAK inhibitors to slow the growth of established metastatic lesions and extend patient survival.

The challenge remains how to best integrate FAK targeting with current and emerging therapies. Ovarian cancer is a complex and heterogeneous disease. Our data indicate that FAK gene

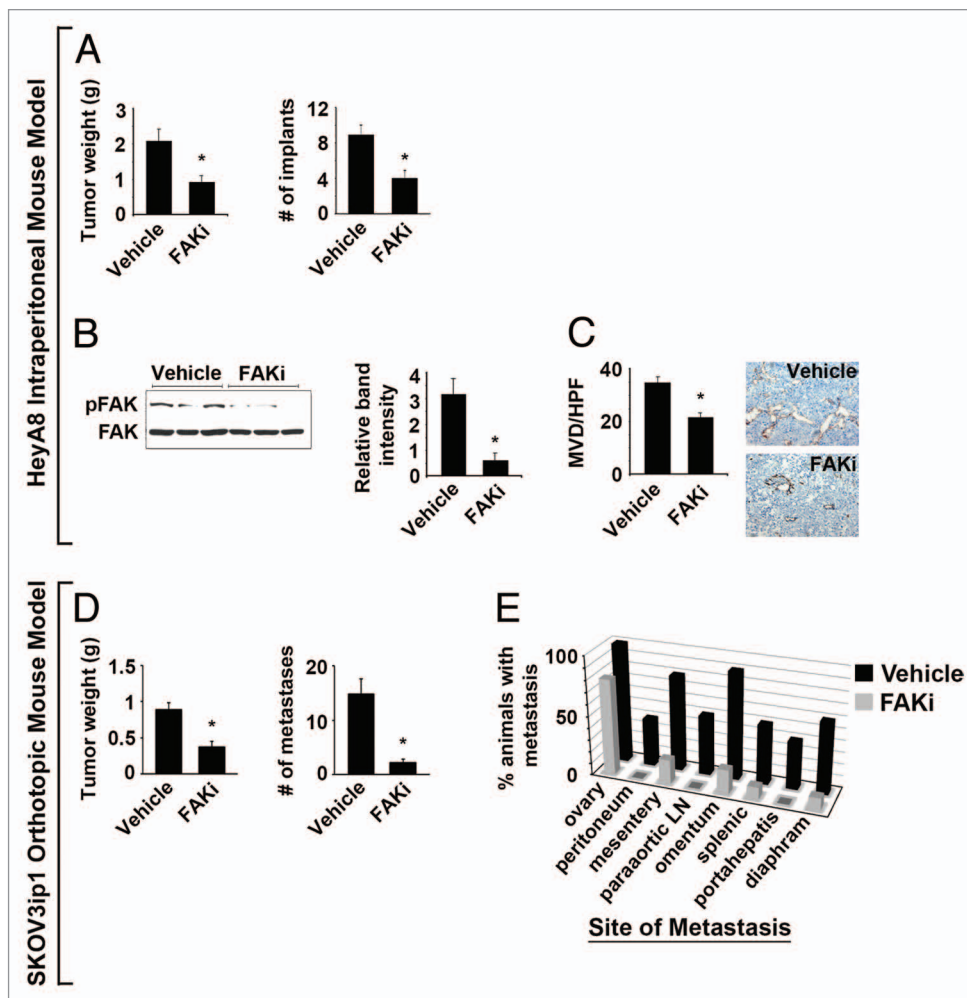


Figure 4. Effect of VS-6062 induced pFAK^{Y397} inhibition on tumor growth and metastasis in HeyA8 intraperitoneal and SKOV3ip1 fully orthotopic mouse models of ovarian cancer. **(A)** Effect of VS-6062 (50mg/kg gavaged BID) on mean HeyA8 tumor weight and number of tumor implants \pm SE. **(B)** Assessment of pFAK^{Y397} expression by western blot to confirm target modulation in VS-6062 treated tumors. The histogram represents mean pFAK^{Y397} relative to total FAK band intensity determined by densitometry \pm SE. **(C)** Mean HeyA8 tumor microvessel density (MVD) evaluated by CD31 immunohistochemical staining (rat anti-mouse CD31 monoclonal antibody, DAKO) following treatment with VS-6062 or vehicle control \pm SE. Representative photomicrographs appear above the histograms. Images were captured at original magnification 200 \times . **(D)** Effect of VS-6062 (50 mg/kg gavaged BID) on mean SKOV3ip1 tumor weight and number of metastases \pm SE. **(E)** Effect of VS-6062 treatment on site-specific metastasis. The histogram displays the percent of animals with persistent ovarian involvement and metastasis to other organ sites following treatment with vehicle control vs. VS-6062. Paraaortic LN, paraaortic lymph nodes; FAKi, FAK inhibitor VS-6062; Vehicle, AEE (sterilized 90% polyethylene glycol 300 and 10% 1-Methyl-2-pyrrolidinone) diluent alone was used for all in vivo experiments.

amplification and overexpression occur in some but not in all cases. Further, FAK was not found to be elevated or activated in a number of cases with increased microvessel density. In these cases, other mediators of angiogenesis (e.g., platelet-derived growth factor, fibroblast growth factor, the polycomb group protein enhance Zeste homolog 2 [EZH2], notch family, the angiotensin [Ang]-TIE system, and the miR-200 family of miRNA) are likely to play a role.^{37,38} There is a small but growing body of literature that initial tumor response to anti-angiogenic therapy may paradoxically be followed by enhanced tumor progression by promoting an invasive phenotype. Experimental models have recently shown that tumors can develop anti-VEGF escape programs associated with metastatic dissemination to lymph nodes and distant sites.^{2,39,40} Whether FAK may be one potential

candidate for molecular targeting of such angioadaptive mechanisms deserves consideration. Furthermore, the present study is fundamentally important for the clinical application of FAK tyrosine kinase inhibitors as it emphasizes that host cells, such as endothelial cells, should be accounted for in the development and characterization of novel biologic agents.

Materials and Methods

Clinicopathological variable analysis

Among the patients included in this analysis ($n = 80$), 83% had advanced stage (III or IV) and 89% had high-grade (III) disease. Eighty-seven percent had serous histology and 62%

underwent optimal surgical cytoreduction. All patients underwent primary surgical cytoreduction and received adjuvant taxane and platinum chemotherapy at MD Anderson Cancer Center (MDACC). Surgical staging was performed according to the International Federation of Gynecology and Obstetrics system. A blinded gynecological pathologist reviewed all specimens. Clinicopathologic data collected with IRB approval included age, stage, grade, histology, extent of surgical cytoreduction (optimal defined as <1 cm residual), disease status, and survival. This study was based on a different cohort of patients than that previously used to establish the clinical relevance of total FAK expression in ovarian carcinoma.¹⁰

Immunohistochemistry

Surgical specimens from the 80 patients were evaluated for FAK and pFAK^{Y397} expression using immunohistochemistry. Formalin-fixed, paraffin-embedded specimens were sectioned at 5 μ m. The specimens were hematoxylin and eosin stained for identification and adjacent sections were used for immunohistochemical staining. Slides were heated overnight at 65 °C and deparaffinized through graded xylenes and ethanol. Antigen retrieval was performed for FAK staining in the Target solution (DAKO Cytomation) under steam for 40 min. Endogenous peroxidase activity was blocked by incubation in 3% hydrogen peroxide in methanol followed by non-specific protein blocking with 5% normal horse serum in phosphate buffered saline (PBS). Sections were incubated overnight at 4 °C with mouse anti-human FAK and pFAK^{Y397} primary antibodies (BD Transduction Laboratories) at 1:25 dilution. Secondary amplification was achieved using the MACH4 polymer-linked horseradish peroxidase (HRP) (Biocare) system. The MACH4 mouse antibody was applied for 20 min, followed by incubation in MACH4 anti-rabbit HRP for 20 min at room temperature. Visualization was achieved with 3,3'-diaminobenzidine (DAB; Open Biosystems). Slides were counterstained with Gill's No. 3 hematoxylin (Sigma-Aldrich), followed by nuclear bluing with PBS. Ovarian cancer cell lines found to express high levels of FAK and pFAK relative to normal ovarian epithelium served as positive controls. Negative controls were established by omitting primary antibody from the staining procedure.

A blinded board-certified pathologist reviewed all sections. FAK and pFAK expression was determined by assessing the distribution and staining intensity of positive tumor cells and tumor-associated endothelial cells. The distribution of positive cells was rated as follows: 0 points, no staining; 1 point, focal or <25%; 2 points, 25–50%; 3 points, 50–75%; 4 points, 75–100%. The staining intensity was rated as follows: 1 point, focal or weak; 2 points, moderate; 3 points, heavy. Points for distribution and intensity were added and an overall score ranging from 0 to 3 was assigned. Each score was categorized into one of four groups. An overall score of 0 was assigned for negative expression of FAK or pFAK if $\leq 5\%$ cells stained, regardless of intensity. An overall score of 1 (1–2 points) designated weak expression of FAK or pFAK, an overall score of 2 (3–4 points) designated moderate expression of FAK or pFAK, and an overall score of 3 (5–7 points) designated FAK or pFAK overexpression.

CD31 immunostaining

Immunohistochemical staining for MVD was performed using mouse anti-human CD31 monoclonal antibody (dilution 1:20, DAKO) on the same specimens as previously described.⁴¹ Tumor MVD was calculated as the average CD31-positive vessel count over 5 sections under x200 high-power fields (HPF). A vessel was defined as an open lumen with 1 or more immediately adjacent CD31-positive cell(s). The optimal, clinically relevant, MVD cut off point associated with death due to disease has been previously established to be 12.7.⁴¹

Quantitative real-time PCR

Enzymatically digested tissue specimens (7 normal ovaries and 10 advanced stage, high-grade serous ovarian cancers) were subjected to negative and positive immunoselection for endothelial cells. The purity of all isolates was tested with endothelial cell markers, P1H12 and von Willebrand factor. Immunopurification yielded endothelial cell purity of >95%. Quantitative real-time PCR was then done on 100 ng of double amplified product from the endothelial cell isolates using primer sets specific for FAK and the housekeeping genes *GAPDH*, *GUSB*, and *cyclophilin*. An iCycler iQ Real-time PCR Detection System (Bio-Rad Laboratories) was used in conjunction with the QuantiTect SYBR Green RT-PCR Kit (Qiagen, Inc.) according to previously described cycling conditions.⁴² To calculate the relative expression of FAK, the $2^{-\Delta\Delta C_T}$ method was used, averaging the C_T values for the three housekeeping genes for a single reference gene value.

Immunofluorescence

Immunofluorescent staining for dual pFAK and CD31 was performed using flash frozen invasive ovarian tumor specimens sectioned at 8 μ m. The tissue was fixed in cold acetone for 10 min followed by non-specific protein blocking with 4% fish gel in PBS for 20 min at room temperature. Sections were incubated overnight at 4 °C with mouse anti-human CD31 (DAKO) at 1:20 dilution. Goat anti-mouse Cy3 (Jackson ImmunoResearch) secondary antibody was applied for 1 h at room temperature. Mouse fragment blocking to prevent secondary antibody cross-reactivity was performed using AffiniPure goat anti-mouse IgG + IgM unconjugated (Jackson ImmunoResearch) at a 1:250 dilution in protein block for 2 h followed by AffinPure F(ab')₂ fragment goat anti-mouse IgG, F(ab')₂ fragment unconjugated (Jackson ImmunoResearch) at a 1:10 dilution in protein block for 2 h. Sections were incubated overnight at 4 °C with mouse anti-human pFAK^{Y397} antibody (BD Transduction Laboratories) diluted 1:100 in protein block and then incubated with goat anti-mouse Cy5 secondary antibody (Jackson ImmunoResearch) for 1 h at room temperature. Nuclear labeling was achieved with a 10 min incubation in Hoechst 33342 stain (Invitrogen) diluted 1:10000 in PBS. Negative controls were established by omitting primary antibody from the staining procedure.

Correlation between FAK gene copy number and expression

We used ovarian sample data posted by TCGA as of February 2009.⁷ Specifically, we used copy number data from CGH arrays run at Memorial Sloan Kettering Cancer Center (MSKCC) and Affymetrix U133A expression arrays run at the Broad Institute. Data were available on both platforms for 38 tumor samples and

10 samples of normal ovary. Paired “normal” CGH data derived from peripheral blood were also available for all of the tumor samples.

For the CGH data, we used the posted “level 3” processed data,⁴³ which reports estimated log ratio values following application of the Circular Binary Segmentation (CBS) algorithm.^{44,45} We focused on the values for chromosome 8, and in particular on the interval from 141 to 143 Mb containing FAK (using coordinates from the UCSC genome browser, build hg18). The average level in this interval was used as to define FAK copy number. After exploration across chromosome 8, we chose a cutoff level of 0.5 for determining gains and losses: CBS values above 0.5 indicate a gain in copy number; values below -0.5 a loss. For all tumor samples, we used the difference between the CBS values for a tumor and its corresponding normal sample (T-N) to assess whether the change was tumor-specific.

The expression array data was quantified using the Robust Multichip Algorithm (RMA).⁴⁶ We focused on the expression levels of the two probesets on the array specifically designed to interrogate FAK: 207821_s_at and 208820_at. We checked for association between levels of the two probes targeting FAK using visual inspection and Pearson correlation. We checked for association between copy number and expression using rank correlation between estimated CBS levels and expression levels of each probeset. We examined this association using all the data (48 samples) and just the tumor data (38 samples). While the positive association between FAK gene copy number and expression was consistently significant using both probesets, we trust the output from probeset 208820_at more because of the relative signal strength; many of the expression levels for 207821_s_at are closer to noise levels. Finally, we used simple regression to estimate the amount of change in expression one would expect to see in response to a unit increase in CBS value using the 208820_at probeset. All computations were performed in the freeware statistical package R, version 2.7.0,⁴⁷ and documented in Sweave.⁴⁸

In vitro experiments

The derivation, source, and maintenance of the human ovarian cancer cell line HeyA8 and human umbilical vein endothelial cells (HUVEC) have been described previously.⁴⁹ VS-6062 (*N*-methyl-*N*-[3-[(2-oxo-2,3-dihydro-1*H*-indol-5-yl)amino]-5-(trifluoromethyl)pyrimidin-4-yl]amino)methyl]pyridine-2-yl)methanesulfonamide; previously known as PF-562,271), generously provided by Pfizer, Inc., is a potent ATP-competitive reversible inhibitor selective for recombinant FAK.¹⁴ VS-6062 is one of several compounds evaluated for biochemical and cellular activities against FAK and was selected for the present investigation based on its potency and specificity for FAK, minimal activity against other kinases tested, and utility for in vitro and in vivo evaluation. To date, VS-6062 has been evaluated in a number of kinase screens/panels and displays >100-fold selectivity against all tested enzymes, excepting some cyclin-dependent kinase (cdk) cyclin complexes. However, the activity of VS-6062 against some cdk in recombinant kinase assays was insufficient to translate into cellular effects. A rigorous in vivo PK/PD evaluation was also completed for VS-6062 by Roberts et al. proving it

to be ideal compound for inhibiting FAK in preclinical models of disease.^{14,15} Accordingly, we treated HeyA8 cells with 0.1–10 μ M VS-6062 for 8 h to determine the in vitro dose kinetics of VS-6062 induced inhibition of pFAK^{Y397}. Whole cell lysate for western blot analysis of FAK and pFAK^{Y397} expression was prepared as previously reported.³⁵ Proteins were separated by 7.5% SDS-PAGE and transferred to nitrocellulose membrane. Membranes were blocked with 5% nonfat milk and incubated with anti-pFAK^{Y397} antibody (1:1000, BD Transduction Laboratories) for 1 h at room temperature. Antibody was detected with 0.167 μ g/mL horseradish peroxidase (HRP)-conjugated anti-mouse secondary antibody (The Jackson Laboratory) and developed with an enhanced chemiluminescence detection kit (Pierce). Membranes were then treated with Restore Stripping Buffer (Thermo Fisher Scientific) for 15 min at room temperature and reprobbed with anti-FAK antibody (1:1000, BD Transduction Laboratories). Time-kinetic experiments were performed to determine the onset and duration of action of VS-6062 in downregulating pFAK^{Y397}. Following treatment with 0.5 μ M of VS-6062, lysates were collected at 1, 8, 12, and 24 h and then analyzed for FAK phosphorylation at residue Y397 by western blot.

To assay cell viability, 2000 HeyA8 cells per well were seeded onto 96-well plates and allowed to adhere overnight. Cells were treated with 0–100 μ M VS-6062 or an equivalent of DMSO vehicle control every 12 h. After 96 h, 50 μ L of 0.15% 3-(4,5-dimethylthiazol-2-yl)-2,5-diphenyltetrazolium bromide was added to each well and incubated for 2 h. The supernatant was removed and cells were dissolved in 100 μ L DMSO. The absorbance at 570 nm was recorded using a FALCON microplate reader and cell viability expressed as percent change relative to control.

Unstimulated HeyA8 cell migration was determined in membrane invasion culture system chambers containing a polycarbonate filter (with 10 μ m pores) that had been soaked in 0.1% gelatin. Both upper and lower wells of the chamber were filled with serum-free RPMI. HeyA8 cells were pretreated with 0.1–1 μ M VS-6062 or vehicle control for 8 h. Single cell suspensions were seeded into the upper wells (5×10^4 cells per well) and incubated at 37 °C for 6 h. Cells that had migrated through the filter into the bottom wells were collected, stained, and counted by light microscopy.⁵⁰ VEGF-A stimulated HUVEC migration was similarly executed. Since it is well known that HUVECs express both FAK and pFAK^{Y397},⁵¹ HUVECs were pretreated with 0.5 μ M VS-6062 or vehicle control for 8 h and then introduced to the membrane invasion culture system (1×10^5 cells per well) with or without the addition of VEGF-A (10 ng mL⁻¹).

For tube formation assays, 50 μ L Matrigel (12.5 mg/mL) was added to each well of a 96-well plate and allowed to solidify for 10 min at 37 °C. The wells were then incubated for 6 h at 37 °C with HUVECs (1×10^4 cells per well), which had been pretreated for 8 h with 0.5 μ M VS-6062 or vehicle control. Cell morphology and count with trypan blue were checked prior to plating the cells on Matrigel to confirm that pretreatment did not affect viability. The formation of capillary-like structures was examined microscopically and photographs were taken using a Retiga

1300 camera and a Zeiss Axiovert S100 microscope. The extent to which capillary-like structures formed in the gel was quantified as previously described.⁴²

In vivo experiments

Female athymic nude (NCR-*nu*) mice were purchased from Taconic Farms Inc. All experiments were supervised by the MDACC Institutional Animal Care and Use Committee. The development and characterization of the mouse models of ovarian cancer used in this investigation have been previously described.^{52,53} For the intraperitoneal model, HeyA8 (0.25×10^6) human ovarian cancer cells resuspended in 200 μ L of Hank's balanced salt solution (HBSS, Mediatech, Inc.) were injected into the peritoneal cavity of female nude mice. For the metastasis-specific orthotopic model, SKOV3ip1 (1.6×10^6) cells were suspended in 30 μ L of HBSS and injected into the right ovary of anesthetized female nude mice through a 1.5 cm intraperitoneal incision. After 8 d, mice were treated with either VS-6062 (50 mg/kg, $n = 14$) or vehicle control ($n = 14$) by gavage every 12 h for 21 d. VS-6062 was suspended in AEE diluent (sterilized 90% polyethylene glycol 300 and 10% 1-Methyl-2-pyrrolidinone) and control mice were treated with AEE diluent alone. Dosing for VS-6062 was based on the results of preliminary dose-response experiments evaluating tumor target modulation in vivo. The weight as well as the number and location of macroscopic tumors were recorded at necropsy. CD31 immunostaining of tumor specimens for MVD quantification was performed as described above. Five random fields at x200 magnification were counted for every specimen. To prepare lysate from tumor specimens for assessment of pFAK^{Y397} target modulation by VS-6062, 0.3 g samples of frozen tumors from 3 control and 3 VS-6062 treated mice were homogenized over ice in radioimmunoprecipitation assay buffer. After incubating the samples on ice for 10 min, they were centrifuged at 4 °C,

14000 rpm for 10 min and the supernatant collected. Protein quantification and western blot for pFAK^{Y397} and total FAK was performed as described above.

Statistical analyses

The Chi-square test was performed to test associations between clinicopathological variables, MVD, and FAK or pFAK expression in both the tumor cells and tumor-associated endothelial cells (SPSS Inc.). Kaplan–Meier survival curves were generated and compared using a 2-sided log rank statistic. Patients who were alive at the last follow-up were censored at the date of last follow-up. The two-tailed Student *t* test was used to test differences in sample means for data resulting from in vitro and in vivo experiments. The Fisher exact test was used to test for differences in metastasis according to treatment group. A *P* value < 0.05 was considered statistically significant.

Disclosure of Potential Conflicts of Interest

No potential conflicts of interest were disclosed.

Acknowledgments

The authors thank Robert R. Langley and Donna Reynolds for helpful discussions and assistance with immunohistochemistry. We would also like to recognize Nicolas Jennings who provided technical expertise in the execution of laboratory experiments. R.L.S., J.B.M., and B.Z. are supported by the NCI T32 Training Grant (CA101642). This research was funded in part by support from NIH Grants (CA110793 and CA109298), the U.T. MD Anderson Cancer Center Ovarian Cancer Spore (P50 CA083639), the Zarrow Foundation, the Betty Ann Asche Murray Distinguished Professorship and the Marcus Foundation to A.K.S., the Ann Rife Cox Chair in Gynecology to R.L.C., and NIH Grants CA-104825 and CA-140933 to S.K.L.

References

- van der Bilt AR, de Vries EG, de Jong S, Timmer-Bosscha H, van der Zee AG, Reyners AK. Turning promise into progress for antiangiogenic agents in epithelial ovarian cancer. *Crit Rev Oncol Hematol* 2012; 84:224-42; PMID:22525643; <http://dx.doi.org/10.1016/j.critrevonc.2012.03.006>
- Páez-Ribes M, Allen E, Hudock J, Takeda T, Okuyama H, Vinals F, Inoue M, Bergers G, Hanahan D, Casanovas O. Antiangiogenic therapy elicits malignant progression of tumors to increased local invasion and distant metastasis. *Cancer Cell* 2009; 15:220-31; PMID:19249680; <http://dx.doi.org/10.1016/j.ccr.2009.01.027>
- Cukierman E, Pankov R, Stevens DR, Yamada KM. Taking cell-matrix adhesions to the third dimension. *Science* 2001; 294:1708-12; PMID:11721053; <http://dx.doi.org/10.1126/science.1064829>
- Chatzizacharias NA, Kouraklis GP, Theocharis SE. Clinical significance of FAK expression in human neoplasia. *Histol Histopathol* 2008; 23:629-50; PMID:18283648
- Mon NN, Ito S, Senga T, Hamaguchi M. FAK signaling in neoplastic disorders: a linkage between inflammation and cancer. *Ann N Y Acad Sci* 2006; 1086:199-212; PMID:17185517; <http://dx.doi.org/10.1196/annals.1377.019>
- Parsons JT, Martin KH, Slack JK, Taylor JM, Weed SA. Focal adhesion kinase: a regulator of focal adhesion dynamics and cell movement. *Oncogene* 2000; 19:5606-13; PMID:11114741; <http://dx.doi.org/10.1038/sj.onc.1203877>
- McLean GW, Carragher NO, Avizienyte E, Evans J, Brunton VG, Frame MC. The role of focal-adhesion kinase in cancer - a new therapeutic opportunity. *Nat Rev Cancer* 2005; 5:505-15; PMID:16069815; <http://dx.doi.org/10.1038/nrcl647>
- Angelucci A, Bologna M. Targeting vascular cell migration as a strategy for blocking angiogenesis: the central role of focal adhesion protein tyrosine kinase family. *Curr Pharm Des* 2007; 13:2129-45; PMID:17627545; <http://dx.doi.org/10.2174/138161207781039643>
- Donninger H, Bonome T, Radonovich M, Pise-Masison CA, Brady J, Shih JH, Barrett JC, Birrer MJ. Whole genome expression profiling of advance stage papillary serous ovarian cancer reveals activated pathways. *Oncogene* 2004; 23:8065-77; PMID:15361855; <http://dx.doi.org/10.1038/sj.onc.1207959>
- Sood AK, Coffin JE, Schneider GB, Fletcher MS, DeYoung BR, Gruman LM, Gershenson DM, Schaller MD, Hendrix MJ. Biological significance of focal adhesion kinase in ovarian cancer: role in migration and invasion. *Am J Pathol* 2004; 165:1087-95; PMID:15466376; [http://dx.doi.org/10.1016/S0002-9440\(10\)63370-6](http://dx.doi.org/10.1016/S0002-9440(10)63370-6)
- Kiechle M, Jacobsen A, Schwarz-Boeger U, Hedderich J, Pfisterer J, Arnold N. Comparative genomic hybridization detects genetic imbalances in primary ovarian carcinomas as correlated with grade of differentiation. *Cancer* 2001; 91:534-40; PMID:11169935; [http://dx.doi.org/10.1002/1097-0142\(20010201\)91:3<534::AID-CNCR1031>3.0.CO;2-T](http://dx.doi.org/10.1002/1097-0142(20010201)91:3<534::AID-CNCR1031>3.0.CO;2-T)
- Hauptmann S, Denkert C, Koch I, Petersen S, Schlüns K, Reles A, Dietel M, Petersen I. Genetic alterations in epithelial ovarian tumors analyzed by comparative genomic hybridization. *Hum Pathol* 2002; 33:632-41; PMID:12152163; <http://dx.doi.org/10.1053/hupa.2002.124913>
- Golubovskaya VM, Nyberg C, Zheng M, Kweh F, Magis A, Ostrov D, Cance WG. A small molecule inhibitor, 1,2,4,5-benzenetetraamine tetrahydrochloride, targeting the y397 site of focal adhesion kinase decreases tumor growth. *J Med Chem* 2008; 51:7405-16; PMID:18989950; <http://dx.doi.org/10.1021/jm800483v>
- Roberts WG, Ung E, Whalen P, Cooper B, Hulford C, Autry C, Richter D, Emerson E, Lin J, Kath J, et al. Antitumor activity and pharmacology of a selective focal adhesion kinase inhibitor, PF-562,271. *Cancer Res* 2008; 68:1935-44; PMID:18339875; <http://dx.doi.org/10.1158/0008-5472.CAN-07-5155>
- Slack-Davis JK, Martin KH, Tilghman RW, Iwanicki M, Ung EJ, Autry C, Luzzio MJ, Cooper B, Kath JC, Roberts WG, et al. Cellular characterization of a novel focal adhesion kinase inhibitor. *J Biol Chem* 2007; 282:14845-52; PMID:17395594; <http://dx.doi.org/10.1074/jbc.M606695200>
- Schultze A, Fiedler W. Therapeutic potential and limitations of new FAK inhibitors in the treatment of cancer. *Expert Opin Investig Drugs* 2010; 19:777-88; PMID:20465362; <http://dx.doi.org/10.1517/13543784.2010.489548>

17. Jones SF, Moore KN, Patel MR, Infante JR, Poli A, Keegan M, Burris HA. A phase I/IB study of paclitaxel in combination with VS-6063, a focal adhesion kinase (FAK) inhibitor, in patients (pts) with advanced ovarian cancer. *J Clin Oncol* [Online] 2013; suppl; abstr TPS2620. Available from: <http://meetinglibrary.asco.org/content/117259-132>
18. Hirt U, Schleicher M, et al. BI 853520, a potent and highly selective inhibitor of protein tyrosine kinase 2 (focal adhesion kinase), shows efficacy in multiple xenograft models of human cancer. *Mol Can Ther* 2011; 10; <http://dx.doi.org/10.1158/1535-7163.TARG-11-A249>.
19. Golubovskaya VM. Targeting FAK in human cancer: from finding to first clinical trials. *Front Biosci (Landmark Ed)* 2014; 19:687-706; PMID:24389213; <http://dx.doi.org/10.2741/4236>
20. Shen TL, Park AY, Alcaraz A, Peng X, Jang I, Koni P, Flavell RA, Gu H, Guan JL. Conditional knockout of focal adhesion kinase in endothelial cells reveals its role in angiogenesis and vascular development in late embryogenesis. *J Cell Biol* 2005; 169:941-52; PMID:15967814; <http://dx.doi.org/10.1083/jcb.200411155>
21. Tavora B, Batista S, Reynolds LE, Jadeja S, Robinson S, Kostourou V, Hart I, Fruttiger M, Parsons M, Hodiava-Dilke KM. Endothelial FAK is required for tumour angiogenesis. *EMBO Mol Med* 2010; 2:516-28; PMID:21154724; <http://dx.doi.org/10.1002/emmm.201000106>
22. Gadducci A, Ferrero A, Cosio S, Zola P, Viacava P, Dompé D, Fanelli G, Ravarino N, Motta M, Cristofani R, et al. Intratumoral microvessel density in advanced epithelial ovarian cancer and its use as a prognostic variable. *Anticancer Res* 2006; 26(5B):3925-32; PMID:17094423
23. Palmer JE, Sant Cassia LJ, Irwin CJ, Morris AG, Rollason TP. Prognostic value of measurements of angiogenesis in serous carcinoma of the ovary. *Int J Gynecol Pathol* 2007; 26:395-403; PMID:17885489; <http://dx.doi.org/10.1097/pgp.0b013e318063bed7>
24. Agochiya M, Brunton VG, Owens DW, Parkinson EK, Paraskeva C, Keith WN, Frame MC. Increased dosage and amplification of the focal adhesion kinase gene in human cancer cells. *Oncogene* 1999; 18:5646-53; PMID:10523844; <http://dx.doi.org/10.1038/sj.onc.1202957>
25. Golubovskaya V, Kaur A, Cance W. Cloning and characterization of the promoter region of human focal adhesion kinase gene: nuclear factor kappa B and p53 binding sites. *Biochim Biophys Acta* 2004; 1678:111-25; PMID:15157737; <http://dx.doi.org/10.1016/j.bbexp.2004.03.002>
26. Santoso JT, Tang DC, Lane SB, Hung J, Reed DJ, Muller CY, Carbone DP, Lucci JA 3rd, Miller DS, Mathis JM. Adenovirus-based p53 gene therapy in ovarian cancer. *Gynecol Oncol* 1995; 59:171-8; PMID:7590467; <http://dx.doi.org/10.1006/gyno.1995.0002>
27. Brower V. Ovarian cancer genome sequencing unveils findings. *J Natl Cancer Inst* 2011; 103:1288-90; PMID:21852263; <http://dx.doi.org/10.1093/jnci/djr346>
28. Tamura M, Gu J, Danen EH, Takino T, Miyamoto S, Yamada KM. PTEN interactions with focal adhesion kinase and suppression of the extracellular matrix-dependent phosphatidylinositol 3-kinase/Akt cell survival pathway. *J Biol Chem* 1999; 274:20693-703; PMID:10400703; <http://dx.doi.org/10.1074/jbc.274.29.20693>
29. Kurose K, Zhou XP, Araki T, Cannistra SA, Maher ER, Eng C. Frequent loss of PTEN expression is linked to elevated phosphorylated Akt levels, but not associated with p27 and cyclin D1 expression, in primary epithelial ovarian carcinomas. *Am J Pathol* 2001; 158:2097-106; PMID:11395387; [http://dx.doi.org/10.1016/S0002-9440\(10\)64681-0](http://dx.doi.org/10.1016/S0002-9440(10)64681-0)
30. Schwock J, Dhani N, Hedley DW. Targeting focal adhesion kinase signaling in tumor growth and metastasis. *Expert Opin Ther Targets* 2010; 14:77-94; PMID:20001212; <http://dx.doi.org/10.1517/14728220903460340>
31. Golubovskaya VM. Focal adhesion kinase as a cancer therapy target. *Anticancer Agents Med Chem* 2010; 10:735-41; PMID:21214510; <http://dx.doi.org/10.2174/187152010794728648>
32. Eisenhauer EL, Abu-Rustum NR, Sonoda Y, Levine DA, Poyner EA, Aghajanian C, Jarnagin WR, DeMatteo RP, D'Angelica MI, Barakat RR, et al. The addition of extensive upper abdominal surgery to achieve optimal cytoreduction improves survival in patients with stages IIIC-IV epithelial ovarian cancer. *Gynecol Oncol* 2006; 103:1083-90; PMID:16890277; <http://dx.doi.org/10.1016/j.ygyno.2006.06.028>
33. Hamilton CA, Miller A, Miller C, Krivak TC, Farley JH, Chernofsky MR, Stany MP, Rose GS, Markman M, Ozols RF, et al. The impact of disease distribution on survival in patients with stage III epithelial ovarian cancer cytoreduced to microscopic residual: a Gynecologic Oncology Group study. *Gynecol Oncol* 2011; 122:521-6; PMID:21683993; <http://dx.doi.org/10.1016/j.ygyno.2011.04.041>
34. Halder J, Landen CN Jr., Lutgendorf SK, Li Y, Jennings NB, Fan D, Nelkin GM, Schmandt R, Schaller MD, Sood AK. Focal adhesion kinase silencing augments docetaxel-mediated apoptosis in ovarian cancer cells. *Clin Cancer Res* 2005; 11:8829-36; PMID:16361572; <http://dx.doi.org/10.1158/1078-0432.CCR-05-1728>
35. Halder J, Kamat AA, Landen CN Jr., Han LY, Lutgendorf SK, Lin YG, Merritt WM, Jennings NB, Chavez-Reyes A, Coleman RL, et al. Focal adhesion kinase targeting using in vivo short interfering RNA delivery in neutral liposomes for ovarian carcinoma therapy. *Clin Cancer Res* 2006; 12:4916-24; PMID:16914580; <http://dx.doi.org/10.1158/1078-0432.CCR-06-0021>
36. Infante JR, Camidge DR, Mileskin LR, Chen EX, Hicks RJ, Rischin D, Fingert H, Pierce KJ, Xu H, Roberts WG, et al. Safety, pharmacokinetic, and pharmacodynamic phase I dose-escalation trial of PF-00562271, an inhibitor of focal adhesion kinase, in advanced solid tumors. *J Clin Oncol* 2012; 30:1527-33; PMID:22454420; <http://dx.doi.org/10.1200/JCO.2011.38.9346>
37. Sood AK, Coleman RL, Ellis LM. Moving beyond anti-vascular endothelial growth factor therapy in ovarian cancer. *J Clin Oncol* 2012; 30:345-7; PMID:22184398; <http://dx.doi.org/10.1200/JCO.2011.38.8413>
38. Pecot CV, Rupaimoole R, Yang D, Akbani R, Ivan C, Lu C, Wu S, Han HD, Shah MY, Rodriguez-Aguayo C, et al. Tumour angiogenesis regulation by the miR-200 family. *Nat Commun* 2013; 4:2427; PMID:24018975; <http://dx.doi.org/10.1038/ncomms3427>
39. Bikfalvi A, Moenner M, Javerzat S, North S, Hagedorn M. Inhibition of angiogenesis and the angiogenesis/invasion shift. *Biochem Soc Trans* 2011; 39:1560-4; PMID:22103487; <http://dx.doi.org/10.1042/BST20110710>
40. Ebos JM, Lee CR, Kerbel RS. Tumor and host-mediated pathways of resistance and disease progression in response to antiangiogenic therapy. *Clin Cancer Res* 2009; 15:5020-5; PMID:19671869; <http://dx.doi.org/10.1158/1078-0432.CCR-09-0095>
41. Lin YG, Han LY, Kamat AA, Merritt WM, Landen CN, Deavers MT, Fletcher MS, Urbauer DL, Kinch MS, Sood AK. EphA2 overexpression is associated with angiogenesis in ovarian cancer. *Cancer* 2007; 109:332-40; PMID:17154180; <http://dx.doi.org/10.1002/cncr.22415>
42. Lu C, Bonome T, Li Y, Kamat AA, Han LY, Schmandt R, Coleman RL, Gershenson DM, Jaffe RB, Birrer MJ, et al. Gene alterations identified by expression profiling in tumor-associated endothelial cells from invasive ovarian carcinoma. *Cancer Res* 2007; 67:1757-68; PMID:17308118; <http://dx.doi.org/10.1158/0008-5472.CAN-06-3700>
43. Mailliard RB, Alber SM, Shen H, Watkins SC, Kirkwood JM, Herberman RB, Kalinski P. IL-18-induced CD83+CCR7+ NK helper cells. *J Exp Med* 2005; 202:941-53; PMID:16203865; <http://dx.doi.org/10.1084/jem.20050128>
44. Olshen AB, Venkatraman ES, Lucito R, Wigler M. Circular binary segmentation for the analysis of array-based DNA copy number data. *Biostatistics* 2004; 5:557-72; PMID:15475419; <http://dx.doi.org/10.1093/biostatistics/kxh008>
45. Venkatraman ES, Olshen AB. A faster circular binary segmentation algorithm for the analysis of array CGH data. *Bioinformatics* 2007; 23:657-63; PMID:17234643; <http://dx.doi.org/10.1093/bioinformatics/btl646>
46. Irizarry RA, Hobbs B, Collin F, Beazer-Barclay YD, Antonellis KJ, Scherf U, Speed TP. Exploration, normalization, and summaries of high density oligonucleotide array probe level data. *Biostatistics* 2003; 4:249-64; PMID:12925520; <http://dx.doi.org/10.1093/biostatistics/4.2.249>
47. Ihaka R, Gentleman RR. A language for data analysis and graphics. *J Comput Graph Stat* 1996; 5:299-314
48. Leisch F. *Compstat 2002 - Proceedings in Computational Statistics*. Physica Verlag, Heidelberg, 2002.
49. Kamat AA, Kim TJ, Landen CN Jr., Lu C, Han LY, Lin YG, Merritt WM, Chaker NS, Gershenson DM, Bischoff FZ, et al. Metronomic chemotherapy enhances the efficacy of anti-vascular therapy in ovarian cancer. *Cancer Res* 2007; 67:281-8; PMID:17210709; <http://dx.doi.org/10.1158/0008-5472.CAN-06-3282>
50. Sood AK, Seftor EA, Fletcher MS, Gardner MJ, Heidger PM, Buller RE, Seftor RE, Hendrix MJ. Molecular determinants of ovarian cancer plasticity. *Am J Pathol* 2001; 158:1279-88; PMID:11290546; [http://dx.doi.org/10.1016/S0002-9440\(10\)64079-5](http://dx.doi.org/10.1016/S0002-9440(10)64079-5)
51. Takahashi M, Berk BC. Mitogen-activated protein kinase (ERK1/2) activation by shear stress and adhesion in endothelial cells. Essential role for a herbimycin-sensitive kinase. *J Clin Invest* 1996; 98:2623-31; PMID:8958227; <http://dx.doi.org/10.1172/JCI119083>
52. Halder J, Lin YG, Merritt WM, Spanuth WA, Nick AM, Honda T, Kamat AA, Han LY, Kim TJ, Lu C, et al. Therapeutic efficacy of a novel focal adhesion kinase inhibitor TAE226 in ovarian carcinoma. *Cancer Res* 2007; 67:10976-83; PMID:18006843; <http://dx.doi.org/10.1158/0008-5472.CAN-07-2667>
53. Shahzad MM, Arevalo JM, Armaiz-Pena GN, Lu C, Stone RL, Moreno-Smith M, Nishimura M, Lee JW, Jennings NB, Bottsford-Miller J, et al. Stress effects on FosB- and interleukin-8 (IL8)-driven ovarian cancer growth and metastasis. *J Biol Chem* 2010; 285:35462-70; PMID:20826776; <http://dx.doi.org/10.1074/jbc.M110.109579>